Monomer Diffusion and the Kinetics of Methyl Methacrylate Radical Polymerization at Intermediate to High Conversion

Alessandro Faldi*,† and Matthew Tirrell

Department of Chemical Engineering and Materials Science, University of Minnesota, Minneapolis, Minnesota 55455

Timothy P. Lodge

Department of Chemistry, University of Minnesota, Minneapolis, Minnesota 55455

Ernst von Meerwall

Department of Physics and Maurice Morton Institute of Polymer Science, The University of Akron, Akron, Ohio 44325

Received January 10, 1994; Revised Manuscript Received May 5, 1994•

ABSTRACT: The diffusion coefficients of a photochromic dye, TTI, and of methyl methacrylate, MMA, have been measured in MMA/poly(methyl methacrylate) (PMMA) solutions by forced Rayleigh scattering and field-gradient NMR, respectively. The polymer concentration was varied from 0 to 80% by weight, and the temperature from −10 to +70 °C. The TTI data could be reduced to values representative of MMA diffusion by taking into account the different sizes of the two molecules. The solution glass transition temperature of MMA/PMMA solutions was also measured between 70 and 100% polymer. The MMA diffusion data are compared to available data and estimates of the propagation rate coefficient and of the initiator efficiency over the same polymer concentration range. Contrary to the general assumption, it is found that propagation is not diffusion controlled. The measured decrease of the propagation rate coefficient requires an explanation different from the one that has traditionally been offered. The comparison between MMA diffusion and initiator efficiency supports the idea that the latter is determined by the mobility of the radical fragments. These observations combined still provide an explanation for the reduction in the overall rate of polymerization, R_p, observed during bulk polymerizations of MMA carried at intermediate to high conversions. The decrease in R_p observed in emulsion polymerization, however, cannot be similarly interpreted. The polymer concentration, w_{pg}, at which an MMA/PMMA solutions turns glassy is compared to the limiting conversion. The limiting conversion correlates well with w_{pg}, but the reason for this is uncertain in light of the above findings.

Introduction

Through numerous studies of bulk free-radical polymerization in the intermediate to high conversion range (i.e., beyond about 50% conversion of monomer into polymer), it is experimentally well established that, for certain monomers and reaction conditions, the overall rate of polymerization decreases drastically with conversion.[1] The rate decrease is much larger than can be attributed to monomer and initiator depletion. The phenomenon has been repeatedly observed when the polymerization temperature was below the glass transition temperature of the pure polymer formed.[1] The decrease of the reaction rate may be so pronounced as to lead to virtual cessation of polymerization at a degree of conversion—the limiting conversion—smaller than 100%.

Without invoking reaction steps in addition to the basic ones—initiation, propagation, and termination—there are essentially three possible causes of a reduced polymerization rate: a decrease in the rate of propagation, a decrease in the initiator efficiency, and a decrease in the decomposition rate of the initiator. The first explanation is the most prevalent in the literature, whereas the second has begun to be discussed more recently; both will be examined in what follows. As for the third possibility, there has been almost no work reported on the kinetics of initiator decomposition during the course of polymerization. For the polymerization of styrene in a 50% solution of toluene, Moad et al.[2] showed that the rate of initiator decomposition was not affected from 0 to 95% conversion of monomer; the initiator used was 2,2′-azobis(2-methylpropanenitrile), commonly known as AIBN. In analyses of polymerization kinetics and in mathematical modeling, the rate of initiator decomposition has invariably been assumed constant. We also assume that the rate of initiator decomposition is constant, and polymerization data obtained under this assumption will be used here.

As most of the available experimental information on propagation kinetics, initiator efficiency, and limiting conversion has been collected for the polymerization of methyl methacrylate (MMA), this system was also selected for the present investigation. Experimental data for ethylene,[3] butyl acrylate,[4] and styrene[5] have recently appeared. Early data of Hayden and Melville[6] for MMA showed a decrease in the propagation rate coefficient, k_p, beyond about 40% conversion. (The measurements actually yielded the product fk_p, where f is the initiator efficiency, but it was assumed that f maintained its initial value throughout the whole range of conversion investigated.) Recently, additional experimental investigations of MMA polymerization have been carried out and k_p has been determined;[7-11] all the studies reported a decrease in k_p beyond some degree of conversion. Although there is agreement among the various studies on the general trend of k_p vs conversion, there are also differences in more detailed features of the decrease, such as the point of onset, its magnitude, and its rapidity. The various experiments were performed under different conditions—e.g., temperature, initiator type, and initiator concentration—and using different experimental techniques.

† Present address: Exxon Chemical Company, P.O. Box 5200, Baytown, TX 77522-5200.

• Abstract published in *Advance ACS Abstracts*, June 1, 1994.

0024-9297/94/2227-4184$04.50/0

It has been widely suggested (e.g., refs 1 and 12) that the observed decrease in k_p is a consequence of the decrease in the mobility of the monomer as the polymer concentration becomes larger. (Conversion and polymer concentration are used interchangeably here.) In this framework, as the polymer concentration increases, the mobility of the monomer diminishes sufficiently to limit the rate of propagation, particularly as the polymerization medium becomes glassy. The assumption of diffusion-controlled propagation has been incorporated into theoretical treatments of the kinetics of polymerization[13-19] by taking k_p to be proportional to the monomer diffusion coefficient. The validity of the assumption has not been assessed in a conclusive way, however, because data on k_p as a function of conversion were scarce until recently and because diffusion data in systems closely resembling the polymerization media were completely lacking. Models have only been compared to overall rate of polymerization and average molecular weight data, which are influenced by many variables simultaneously. It has been pointed out[19] that some models produced values of k_p orders of magnitude lower than experimentally observed.[7] The disagreement was ascribed to the failure of the models to account for a decreasing f; the underlying assumption of diffusion-controlled propagation was not challenged.[19] In the following, the notion of diffusion-controlled propagation will be tested directly by comparing k_p to monomer diffusion data.

At a given polymerization temperature, the limiting conversion, X_l, has been identified as the conversion at which the polymerization medium becomes a glass. The first indication came from the observation that raising the temperature of MMA polymerization close to the glass transition temperature of the formed polymer in its bulk state could lead to complete conversion.[20,21] Subsequently, also for the polymerization of MMA, Horie et al.[22] used an expression based on free volume theory[23] to estimate the conversion at which the medium turned into a glass and found that it correlated well with the limiting conversion. In no case, however, have experimental data on the glass transition been compared to the observed limiting conversions. The comparison is also made in this work.

The accepted explanation for the cessation of polymerization at X_l is also connected to the monomer mobility. It is argued that the monomer is essentially immobile in the glassy environment and thus polymerization ceases. (The argument clearly assumes the validity of the connection between X_l and the medium glass transition.) Recent measurements of the diffusion coefficient of small tracer molecules in glassy polymer solutions[24] have showed that although the tracer mobility is small, it is not zero. Below, we use MMA diffusion data to test whether the monomer mobility is small enough to explain a near-zero polymerization rate.

It is important to point out that no limiting conversion was observed in a study of the emulsion polymerization of MMA[7] whereas it has repeatedly been observed for bulk polymerization—e.g., refs 6, 9, 11, and 25–28—even at temperatures higher than the one used in the emulsion study. Another important difference between bulk and emulsion polymerization is that the high-conversion values of k_p measured in bulk are orders of magnitude lower than those measured in emulsion at the same polymer concentration.[12] Russell et al.[19] have argued that these differences are a consequence of a drastic, and unaccounted for, reduction of the initiator efficiency as conversion increases during bulk polymerization. No such reduction is expected during emulsion polymerization since the initiator is located in the aqueous phase, which is essentially unchanged throughout the process. These authors have attributed the decrease of f to the reduced mobility of the initiator fragments as the polymer concentration increases, which would, in turn, greatly enhance the probability that the fragments undergo recombination before they have a chance to move apart following the scission of the initiator.

Historically, the dependence of f on polymer concentration has been the object of relatively little experimental investigation. Until recently, measurements of f have been discordant; one showed a constant efficiency[29] whereas others[30,31] reported a decrease of f with conversion. More recent measurements have all revealed a decrease in f as the polymer concentration increased during the solution polymerization of styrene[2] and the bulk polymerization of MMA.[9,32] Estimates from kinetic data of MMA bulk polymerization also showed a rapid decrease of f with increasing polymer concentration.[19] Modeling of bulk polymerization has largely been conducted assuming that f was constant, although the suggestion that this might not be the case has been made.[14] Some theoretical efforts[18,32,33] have included an analysis of f as a function of the course of polymerization; the guiding principle has been that a reduced mobility of the initiator fragments would increase the chances of recombination and thereby reduce f. In the following, the polymer concentration dependence of f, from both experiment and calculation, is compared to the concentration dependence of the diffusion coefficient of MMA. Since, as will be shown, MMA is rather similar in size—and in some cases also in shape—to the initiator fragments, the comparison will be a basic test of the assumption of diffusion-limited initiation kinetics.

Experimental Section

Materials. Poly(methyl methacrylate) (PMMA) was obtained from Polymer Laboratories. Three samples of narrow dispersity ($\bar{M}_w/\bar{M}_n < 1.1$) and size exclusion chromatography peak molecular weight, M_p, equal to 7×10^4 (PMMA-70), 1.27×10^5 (PMMA-127), and 4.8×10^5 (PMMA-480), were dissolved in benzene, filtered through a Nylon-66 syringe filter unit with a pore size of 0.45 μm, and freeze-dried.

Methyl methacrylate, obtained from Aldrich Chemical Co., was successively washed three times with a 10% solution of sodium hydroxide, once with water, three times with a saturated solution of sodium metabisulfite, once with water, and subsequently dried over magnesium sulfate and calcium hydride. It was then stirred with fresh calcium hydride for 12–18 h and finally distilled over calcium hydride under a reduced pressure of dry nitrogen; partial polymerization occurred during distillation. The monomer was always used immediately after purification.

Inhibitor. 2,6-Dichlorobenzoquinone (DCBQ) was obtained from Kodak and used as received.

2-(4,5-Dihydro-4,4-dimethyl-3(2*H*)-oxo-2-thienylidene)-4,5-dihydro-4,4-dimethyl-3(2*H*)-thiophenone, a photochromic dye hereafter referred to as TTI, was synthesized in good yield following procedures published in the literature.[34,35] Melting point determination, gas chromatography, and ^{1}H NMR confirmed that the product obtained was pure TTI.[36] Some properties of the TTI dye have been summarized before[37] and will be repeated here. The dye undergoes reversible *trans* ↔ *cis* isomerization in different environments, without any side reactions. TTI is considered to have high thermal stability—no decomposition below 360 °C—with the thermal *cis* → *trans* isomerization starting around 160 °C. It was found, however, that prolonged heating of a solution of TTI in the presence of oxygen destroys the dye.[37]

Sample Preparation. All samples for forced Rayleigh scattering (FRS) were prepared in 2-mm path length spectroscopic cells to which glass tubes were attached. Freeze-dried PMMA was added to the cells, followed in order by a solution of TTI in

MMA and a solution of DCBQ in MMA. The solutions were filtered through a Nylon-66 syringe filter unit with a pore size of 0.2 μm. After an initial rough homogenization, the cells were placed under vacuum to evaporate MMA until the desired concentration was reached. Some of the more concentrated samples required an increase in temperature to evaporate the necessary quantity of MMA in a reasonable amount of time. Once the appropriate final concentration was reached, the cells were cooled to −30 °C, flame-sealed under dry nitrogen, and then placed in an oven to homogenize completely. The oven temperature varied according to the polymer concentration of the samples; temperatures between 70 and 120 °C were used. The ratio of inhibitor to monomer necessary to prevent polymerization during homogenization was determined by carrying out separate tests. The degree of sample homogeneity was checked by measuring the dye diffusion coefficient at various locations in the cells; when the measurements were within 10% of one another, the samples were deemed homogeneous. Following the procedure detailed above, solutions having polymer concentrations, w_p, between 40 and 81% by weight, TTI concentrations between 0.4 and 0.6%, and inhibitor-to-monomer ratios between 0.4 and 3% were prepared. The combined amounts of TTI and DCBQ never exceeded 1% of the total weight. For the majority of the samples the polymer used was PMMA-70, but a few samples were prepared with PMMA-127 and PMMA-480.

The samples for field-gradient nuclear magnetic resonance (FG-NMR) measurements were prepared as follows. Appropriate NMR tubes were made in-house according to the requirements of the spectrometer used. Solutions of PMMA in benzene with a polymer concentration of about 5% were filtered into the NMR tubes and freeze-dried. A solution of DCBQ in MMA was then added. The rest of the procedure was analogous to the one used for the FRS samples. In this way samples containing 0–70% polymer and an inhibitor-to-monomer ratio between 0.4 and 3% were prepared. The amount of inhibitor used was at most 1% of the total weight. All samples were prepared using PMMA-70.

Forced Rayleigh Scattering. The basic concepts behind the FRS method have been recently reviewed.[38,39] In this work, the amplitude-grating protocol was used: the grating was created by an Ar^+ laser operating at $\lambda_0 = 488$ nm and was probed using the same laser attenuated by a factor of 10^4. The optical configuration of the FRS apparatus and the data acquisition procedure have been described elsewhere.[36]

All the FRS decay curves could be fit to a single-exponential function:

$$I(t) = (Ae^{-t/\tau} + B)^2 + C^2 \quad (1)$$

where I is the measured intensity, A is a prefactor, t is the time, τ is the characteristic decay time, B is a coherent baseline term, and C is an incoherent baseline term. The diffusion coefficient was determined from values of τ obtained at different grating spacings according to the following relation:

$$\frac{1}{\tau} = \frac{4\pi^2 D_{TTI}}{d^2} + \frac{1}{\tau_0} \quad (2)$$

where D_{TTI} is the diffusion coefficient of TTI, d is the grating spacing, and $1/\tau_0$ is the intercept. A typical decay curve for a sample containing 81% PMMA-70, 18% MMA, 0.3% DCBQ, and 0.5% TTI (all concentrations by weight) is displayed in Figure 1 together with the dependence of $1/\tau$ on $1/d^2$ in the inset. The linearity of the data in the inset confirms that a diffusion process is being monitored by the FRS decay. Measurements were performed between −10 and +70 °C, at 10 °C intervals, and with a precision of ±0.1 °C.

Field-Gradient NMR. Measurements of the MMA center-of-mass diffusion coefficient were performed using the large-pulsed-gradient spin-echo method pioneered by Stejskal and Tanner.[40] The implementation used in this work has been described in detail elsewhere.[41–43] Nonspectroscopic pulsed ^1H NMR was performed at 33 MHz in a conventional electromagnet. The attenuation of the principal spin echo at a time $2\tau = 50$ ms was measured as a function of the duration, δ, of two field-gradient pulses of magnitude G near 135 G/cm. (The value of G depended slightly on temperature and was calibrated to within 1.5%.) The value of δ was varied in 10–15 steps from zero until the echo amplitude had decreased below 2% of its original value but never exceeded 16 ms. Any δ-dependent differential gradient pulse length correction to keep the echo centered at 2τ, as well as any attendant receiver phase adjustments, proved to be unnecessary at this modest gradient strength. To narrow and stabilize the spin echo, a steady field gradient of 0.85 G/cm was also applied throughout each measurement. The echo amplitude was averaged over 6–20 measurements.

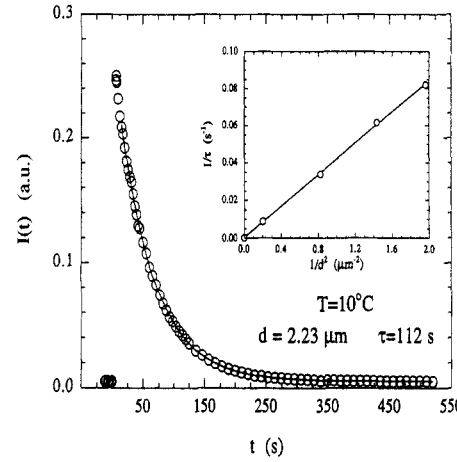

Figure 1. Measured FRS decay curve from a solution with $w_p = 81\%$. The smooth line is a nonlinear fit to eq 1. The linear relationship between the inverse decay time and the inverse square of the grating spacing, according to eq 2, is shown in the inset.

The experiments were optimized for the measurement of MMA diffusion. Nevertheless, at 30.5 and 50.5 °C, the diffusion coefficient of PMMA was also measurable between 6 and 32% polymer. Primary data reduction was performed off-line using software described elsewhere.[44] The correction for the effect of residual field gradients[45] was also performed but had a negligible effect.

For pure MMA, a single diffusion rate described the data well. When both MMA and PMMA diffusion were evident, the echo attenuation data were fitted by a sum of two exponential functions;[44] the two different diffusion rates and the fractional amplitude of the faster-diffusing component were adjusted to provide the best fit. The smaller rate was postulated to have a small distribution as suggested by the narrow polydispersity of the polymer sample; this procedure is based on the well-understood connection between diffusivity and molecular weight for polydisperse polymers in solution.[46] When the presence of a slower component was discernible in the spin echo, but without the possibility of measuring its diffusion rate, the data were fitted using a single rate—characteristic of MMA diffusion—plus an essentially unattenuable echo fraction.[44]

At 50 °C, a sample with $w_p = 70\%$ produced the results shown in Figure 2, which displays the natural logarithm of the spin echo amplitude, A, normalized by A_0, the echo amplitude in the absence of the field gradient, plotted against the combined gradient parameters $\delta^2G^2(\Delta - \delta/3)$, where Δ is the time between the gradient pulses. The echo data could be described by the following expression:

$$A/A_0 = h + (1 - h)\exp[-\gamma^2 D_{MMA}\delta^2 G^2(\Delta - \delta/3)] \quad (3)$$

where γ is the magnetogyric ratio of the ^1H nuclide, D_{MMA} is the diffusion coefficient of MMA, and h is the unattenuable fraction of the echo. Measurements were performed at four temperatures between −9.5 and +50.5 °C, at 20 °C intervals, and with a precision of ±0.2 °C.

Solution Glass Transition. The glass transition temperatures of the three PMMA samples used in this work were measured with a Perkin-Elmer DSC7 differential scanning calorimeter at different heating rates. A calibration was performed with indium at each heating rate, and at least three runs were carried out to

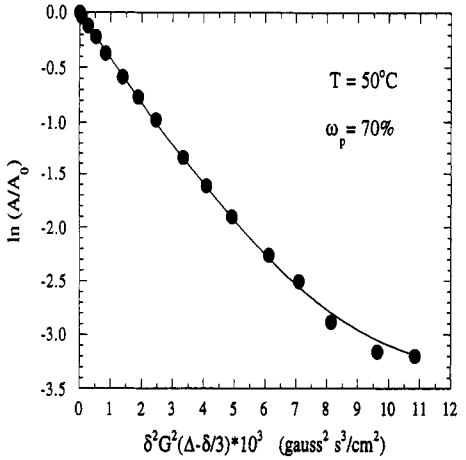

Figure 2. Plot of the normalized spin echo intensity against a combination of gradient parameters. The solid line is the best fit to eq 3.

check reproducibility. The glass transition was taken as the intersection of the baseline and the sloping part of the heating trace. The transition point was determined with a precision of ±1 °C. The measured glass transition temperatures were independent of heating rate and of molecular weight.[36] The average glass transition temperature of all three polymers was 119 ± 1 °C.

The solution glass transition temperature, T_{gs}, was measured for some of the FRS samples. All measurements were performed using a Perkin-Elmer DSC7 differential scanning calorimeter and Perkin-Elmer high pressure capsules. The experimental protocol was analogous to the one detailed above. For each sample, the measured glass transition temperature increased linearly with increasing heating rate; the "true" glass transition temperature was determined as the extrapolated value to zero heating rate.[36]

Results

Using free-volume theory, all the D_{TTI} data obtained from FRS can be scaled in such a way as to represent the diffusion coefficients of MMA under the same conditions of polymer concentration and temperature; the procedure is as follows. The Vrentas–Duda[47] free-volume model of small-molecule diffusion in binary polymer/solvent solutions has been extended to ternary solutions of a polymer and two small molecules.[48] A prediction of the extended model is a linear relationship between the logarithms of the diffusion coefficients of the two small molecules, provided one is present in trace amounts.[49] When applied to the particular case discussed here, the above results imply

$$\log D_{TTI} = \xi_{ts} \log D_{MMA} + \beta \qquad (4)$$

where ξ_{ts} is a parameter that represents the ratio of the sizes of the TTI and MMA molecules and β is the intercept.

To verify whether eq 4 is followed in the present system, diffusion data for TTI and MMA obtained for samples with identical polymer concentrations and temperatures are required; some FRS and FG-NMR data were collected under conditions that very nearly satisfy this requirement. However, since diffusion data are rather sensitive to polymer concentration and temperature, the small mismatches in the concentration of the FRS and FG-NMR samples and in the temperature of the measurements resulted in some scatter when D_{TTI} and D_{MMA} were plotted according to eq 4, which compromised a precise assessment of the validity of the equation. To eliminate this problem,

Table 1. Vrentas–Duda Free-Volume Parameters

$\hat{V}_1^*$ (cm³/g)	0.87[a]
$\hat{V}_2^*$ (cm³/g)	0.757[b]
$(K_{11}/\gamma) \times 10^3$ (cm³/g·K)	0.815[c]
K_{21} (K)	143[c]
$(K_{12}/\gamma) \times 10^3$ (cm³/g·K)	0.477[d]
K_{22} (K)	52.38[d]
T_{g1} (K)	143[e]
T_{g2} (K)	392[f]
a	0.44[g]

[a] Reference 51. [b] References 51 and 52. [c] From the temperature dependence of MMA viscosity in ref 53. [d] From the WLF constants in ref 37. [e] Reference 54. [f] This work. [g] From PMMA thermal expansion data in ref 55.

the FG-NMR data were interpolated using a modified Vrentas–Duda expression:

$$\log D_{MMA} = \log D^\circ - \frac{E}{2.303RT} - \frac{1}{2.303}\left\{\frac{(1-w_2)\hat{V}_1^* + \xi w_2 \hat{V}_2^*}{\hat{V}_f/\gamma}\right\} \qquad (5)$$

$$\frac{\hat{V}_f}{\gamma} = (1-w_2)\left(\frac{K_{11}}{\gamma}\right)(K_{21} + T - T_{g1}) + w_2\left(\frac{K_{12}}{\gamma}\right)[K_{22} + a(T - T_{g2})] \qquad (6)$$

where D° is a preexponential factor, E is the activation energy, R is the gas constant, T is the temperature, w_2 is the weight fraction of PMMA, $\hat{V}_1^*$ and $\hat{V}_2^*$ are the specific volumes of MMA and PMMA at 0 K, respectively, ξ is a size parameter, $\hat{V}_f/\gamma$ is the solution free volume, (K_{11}/γ), K_{21}, (K_{12}/γ), and K_{22} are free-volume parameters, T_{g1} and T_{g2} are the glass transition temperatures of MMA and PMMA, respectively, and a is described below. In applying eqs 5 and 6 to the FG-NMR results, the contribution of DCBQ to the free volume was assumed to be the same as that of MMA. Three parameters, D°, E, and ξ, were adjusted to fit eq 5 to the FG-NMR data whereas the other parameters—reported in Table 1—were obtained according to Vrentas and co-workers[47,50] from properties of the pure components. The parameter a requires further comment; it does not appear in the original formulation of the free-volume model by Vrentas and Duda[47] but is introduced here for the following reason. The polymer free-volume parameters, (K_{12}/γ) and K_{22}, are invariably obtained from measurements carried out above T_{g2}; their extrapolation to lower temperatures may lead to a negative polymer free volume.[24] In the present case a negative polymer free volume would be obtained below 66.5 °C using the Vrentas–Duda original formulation with the value of the polymer free-volume parameters reported in Table 1. For this reason the parameter a is introduced and estimated as the ratio of the coefficients of thermal expansion of the polymer below and above T_{g2}, respectively; this addition gives a zero polymer free volume at 0 °C. A procedure analogous to the one reported here has been used previously.[24]

The free-volume expressions, eqs 5 and 6, can now be used to calculate D_{MMA} in solutions of exactly the same concentration and at the same temperature as the solutions in which D_{TTI} was measured. Figure 3 displays the measured D_{TTI} values and interpolated D_{MMA} values obtained according to the procedure detailed above. From a linear fit to the data in Figure 3, the values of the parameters in eq 4 can be extracted: $\xi_{ts} = 1.86$ and $\beta = 4.25$. The parameter ξ_{ts} can also be estimated from the values of the molar volumes of TTI and MMA at 0 K obtained following Haward;[51] the procedure gives ξ_{ts} =

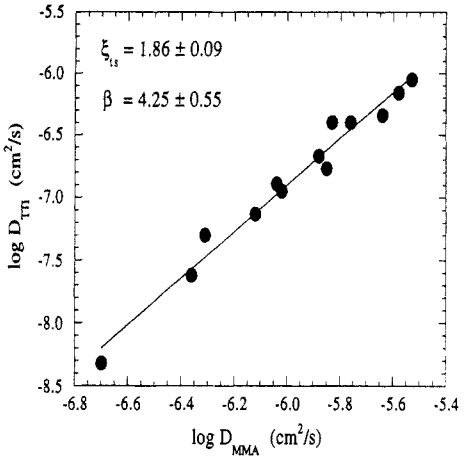

Figure 3. Plot of log D_{TTI} vs log D_{MMA}. The straight line is the best linear fit to the data according to eq 4. The values of the parameters obtained from the fit are shown together with their confidence intervals.

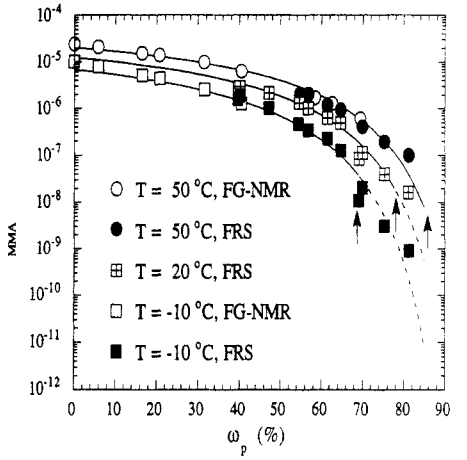

Figure 4. Values of D_{MMA} as a function of polymer concentration, w_p, for three temperatures. The solid lines are calculated from eqs 5 and 6 using the parameters in Tables 1 and 2. The arrows indicate the glass transition at each temperature.

Table 2. Vrentas–Duda Fitted Parameters

$D°$ (cm²/s)	1.61×10^{-3}
E (cal/mol)	778
ξ	0.60

2.22, in reasonable agreement with the value extracted from the diffusion data. Equation 4 can then be used to scale all the D_{TTI} values to the D_{MMA} values that would have been obtained, had measurements been performed under the same conditions. Hereafter, whenever reference will be made to D_{MMA}, it should be intended as including both the values obtained from scaling of D_{TTI} data according to eq 4 and the values measured by FG-NMR.

The dependence of D_{MMA} on polymer concentration at three temperatures is illustrated in Figure 4. The arrows indicate the glass transition at each temperature (vide infra). The solid lines are values from eqs 5 and 6 obtained using the parameters in Table 1 and adjusting $D°$, E, and ξ to give the best fit of D_{MMA} at all the temperatures and concentrations available, with the exclusion of the data for glassy solutions since the Vrentas–Duda model—in the form of eqs 5 and 6—is valid only up to the glass transition. The extension of the model predictions into the glassy regions are nevertheless shown in Figure 4 as dashed lines. The fitted parameters are reported in Table 2.

It was verified that D_{MMA} is independent of PMMA molecular weight by carrying out measurements using

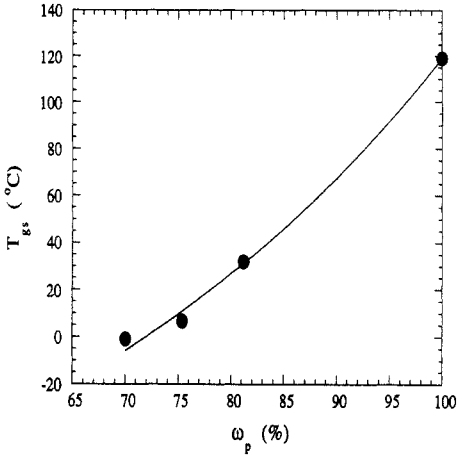

Figure 5. Solution glass transition temperature as a function of polymer concentration, w_p. The line is the best fit to eq 7.

PMMA-127 (w_p = 40 and 69%) and PMMA-480 (w_p = 55%).[36] Since PMMA of molecular weight above 5×10^4 shows a constant glass transition temperature,[56] this behavior is expected. The D_{MMA} values displayed in Figure 4 include the data for all the PMMA molecular weights.

The effect of ageing on the "glassy" data in Figure 4 is not known and was not investigated. The glass transition temperature was crossed very slowly; typical rates were between 0.5 and 1 °C/h. The "quenches" below the glass transition were also performed at similar rates.

The solution glass transition temperature, T_{gs}, is plotted in Figure 5 as a function of w_p including bulk PMMA; the solid line is the fit to the Kelley and Bueche relation:[23]

$$T_{gs} = \frac{\alpha_1(1-\phi_2)T_{g1} + \alpha_2\phi_2 T_{g2}}{\alpha_1(1-\phi_2) + \alpha_2\phi_2} \tag{7}$$

where ϕ_2 is the polymer volume fraction and α_1 and α_2 are the differences between the thermal expansion coefficients above and below the glass transition temperatures of MMA and PMMA, respectively. The value of α_2 can be found from literature data[55] for PMMA ($\alpha_2 = 3.21 \times 10^{-4}$ K^{-1}) whereas α_1 is found by fitting eq 7 to the data in Figure 5 ($\alpha_1 = 5.76 \times 10^{-4}$ K^{-1}). (The volume fraction and weight fraction values are easily interchanged by assuming ideal mixing.) On setting T_{gs} equal to the temperature of the diffusion measurements in eq 6, the polymer concentration at which the solution becomes glassy, w_{pg}, can be estimated; the positions of the arrows in Figure 4 were determined according to this procedure.

Discussion

First, the question of whether propagation is diffusion-controlled will be addressed using the D_{MMA} data presented here and the k_p data presented in the literature.[6,7,9-11] A convenient way to frame the problem follows the Smoluchowski theory of diffusion-controlled reactions,[57] which, when applied to propagation, gives

$$k_p = 4\pi b D_{MMA} \tag{8}$$

where b is the so-called capture radius, the distance below which the reaction occurs instantaneously. For eq 8 to be followed and to make physical sense, it is necessary that k_p and D_{MMA} have a similar concentration dependence beyond the point of onset of diffusion control, X_c. (For each set of k_p data used here, X_c is chosen, somewhat arbitrarily, as the polymer concentration at which k_p starts to decrease.) It is also required that b have a physically

Table 3. Estimates of b at X_c

T (°C)	X_c (%)	b (Å)	ref
22.5	40	2.53×10^{-6}	6[a]
0	60	8.27×10^{-6}	9
60	76	23.6×10^{-6}	11
50	84	77.6×10^{-6}	7[b]
70	87	398×10^{-6}	10[c]

[a] Used D_{MMA} datum at T = 20 °C. [b] Used D_{MMA} datum at w_p = 81%. [c] Used D_{MMA} from eqs 5 and 6 with T_{g2} = 105 °C.

reasonable value, certainly not larger than the size of a polymer chain or much smaller than the size of MMA. To satisfy these two requirements would strongly support the notion of diffusion-controlled propagation.

A detailed comparison of the concentration dependence of k_p and D_{MMA} beyond X_c and up to the highest concentrations for which k_p data are available was made elsewhere.[36] In some cases the comparison required using the Vrentas–Duda model to extrapolate the D_{MMA} data. The agreement of the concentration dependence of k_p and D_{MMA} ranged from very good to rather poor. The kinetic data from bulk polymerization[6,9-11] showed a concentration dependence similar to or steeper than that of D_{MMA}, whereas the emulsion polymerization data[7] showed a weaker dependence. Overall, when all the k_p data were examined, no definitive statement could be made as to whether k_p and D_{MMA} had the same concentration dependence; it could only be concluded that the dependence was rather similar in some cases.

Table 3 shows the values of b at X_c calculated by inserting the appropriate k_p and D_{MMA} in eq 8; in no case is a physically reasonable value of b obtained. When the calculations were carried out at concentrations beyond X_c, values of b on the same order of magnitude as, or smaller than, those reported in Table 3 were obtained using the bulk polymerization data.[6,9-11] Notice that in two cases, at T = 22.5 °C and T = 0 °C—kinetic data from refs 6 and 9, respectively—both k_p and D_{MMA} data are available up to w_{pg}, but the values of b calculated at the glass point were close to, or smaller than, those reported in Table 3. (The D_{MMA} values at T = 20 °C were compared to the k_p data at T = 22.5 °C without any correction for the temperature difference.) Using the k_p data from emulsion polymerization[7] beyond X_c gave higher, but still unreasonable, b values; this behavior was due to the weaker concentration dependence of k_p compared to D_{MMA}.

The egregious quantitative failure of eq 8 in the range of polymer concentrations for which k_p and D_{MMA} data are available implies that the kinetics of propagation are not controlled by the diffusion of MMA. To recast the conclusion more in the language of chemical kinetics, for all the measured values of D_{MMA} and a reasonable value of b, say 5 Å, the number of collisions between the reactants—proportional to the right-hand side of eq 8—is very much higher than the number of collisions necessary for the reaction to occur—proportional to k_p. This remains true at w_{pg} and thus refutes the conventional notion that the near-zero rate of propagation observed at the glass transition is attributable to the small mobility of MMA there. Finally, given the magnitude of b extracted from eq 8, one is led to infer that no refinement in the theory of diffusion-controlled reactions that maintains the proportionality between k_p and D_{MMA} will change the above conclusions. Values of D_{MMA} many orders of magnitude lower than those measured in this study would be necessary to support the notion of diffusion-controlled propagation.

The conclusion reached above does not rule out completely the possibility that propagation may become controlled by diffusion, but it does imply that, as far as the polymerization of MMA is concerned, conversions higher than those explored thus far must be reached to realize such a condition. (An indication of this might be found in the b values in Table 3, which become "more reasonable" at higher values of X_c.) Suggestions that propagation might not be controlled by monomer diffusion have been made previously,[14,58] but in an indirect fashion because of the lack of monomer diffusion data. Evidence for a diffusion-controlled polymer–small molecule reaction has been presented recently by Gebert et al.[59] in a study of phosphorescence quenching, but the rate constant involved was on the order of 10^9 L mol^{-1} s^{-1}, about 7 orders of magnitude higher than the values of k_p typical of MMA polymerization. Having shown that propagation is not controlled by MMA diffusion in the range of polymer concentration investigated, the issue arises of how to interpret the experimentally observed decrease of k_p at intermediate to high conversions; no answer will be offered here.

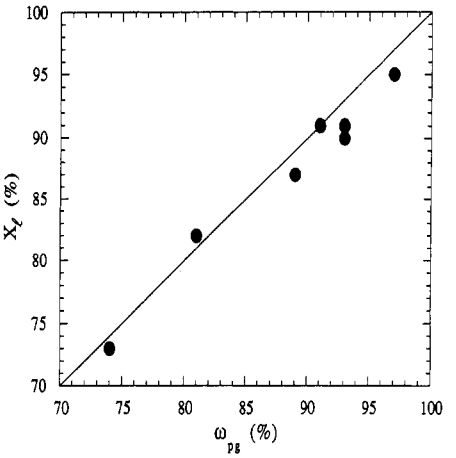

Figure 6. Correspondence between the limiting conversion, X_l, and the glass transition concentration, w_{pg}. The X_l data are from refs 6, 9, 11, 26, and 60.

The values of w_{pg} obtained from eq 7—using T_{g2} = 105 °C[60]—are compared in Figure 6 with the X_l values obtained from the literature for the polymerization of MMA.[6,9-11,26,61] (In the kinetic studies used for the comparison in Figure 6, the course of polymerization was followed using a variety of experimental methods and all revealed the existence of a limiting conversion.) The agreement between w_{pg} and X_l is rather satisfactory, especially considering the experimental uncertainties as well as the fact that the polymerization media and the MMA/PMMA solutions considered here are not completely equivalent systems. Although the connection between the limiting conversion and the medium glass transition is not new,[22] this is the first time the connection has been made using experimental T_{gs} data for a system closely resembling the one encountered during MMA polymerization.

The task is thus to understand the origin of the apparent connection between the limiting conversion and the glass transition. The explanation based on a drastic reduction of the diffusivity of MMA at w_{pg}—leading to a near-zero rate of propagation—must be abandoned in light of the previous comparison between MMA diffusion and propagation kinetics.

The initiator efficiency of dimethyl 2,2′-azobis(methyl 2-methylpropanoate) (AIBME) was measured as a function of polymer concentration during the polymerization of MMA at 60 °C by Shen et al.[32] and is compared to D_{MMA} in Figure 7. All data in Figure 7 are for polymer concentrations well below w_{pg} = 91%. The agreement between the two sets of data is not perfect, especially at

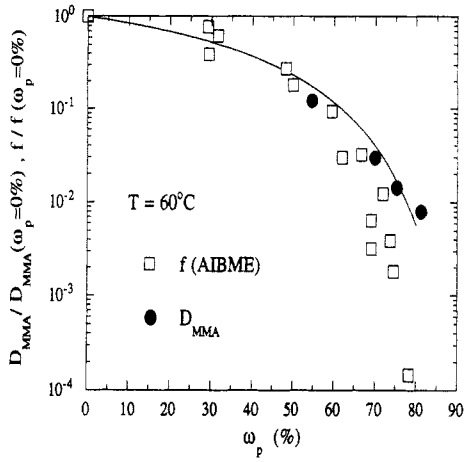

Figure 7. Comparison of the polymer concentration dependence of D_{MMA} with that of f for AIBME. The initiator efficiency data are from ref 32. The solid line is calculated from eqs 5 and 6 using the pararmeters in Tables 1 and 2. The diffusion coefficient and efficiency data are normalized with respect to their values at $w_p = 0\%$.

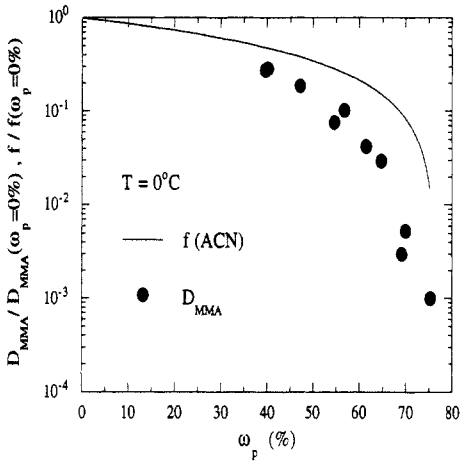

Figure 8. Comparison of the polymer concentration dependence of D_{MMA} with that of f for ACN. The solid line is obtained from the expression used in ref 9 to interpolate the f data. The diffusion coefficient and efficiency data are normalized with respect to their values at $w_p = 0\%$.

high polymer concentrations, but there is a strong similarity in the concentration dependence of f and D_{MMA}. It should be noted that over the polymer concentration range for which values of both quantities are available, the decrease in f and D_{MMA} is about 2 orders of magnitude, not a negligible amount. The chemical structure of the AIBME radical fragment is very similar to that of MMA, as is its size and shape—the size ratio of the AIBME radical to MMA is 0.98, from ref 51. Therefore, the diffusion coefficient of the AIBME fragment is expected to be very well represented by D_{MMA}. The very similar concentration dependence of f and D_{MMA} is consistent with the idea that the behavior of f is determined by the diffusivity of the radicals.

The efficiency of 1,1′-azobis(cyclohexanecarbonitrile) (ACN) from the data of Sack et al.[9] for the polymerization of MMA at 0 °C are compared to D_{MMA} in Figure 8. (The interpolating equation given by Sack et al.[9] is used instead of the actual data.) In this case, $w_{pg} = 74\%$ and the data extend up to the glass transition. Despite a less-than-perfect quantitative agreement between the two sets of data, the polymer concentration dependence is similar. An estimate of the ratio of the size of the ACN radical to the size of MMA according to Haward[51] gives a value of 1.17, which again makes D_{MMA} a reasonable estimate of

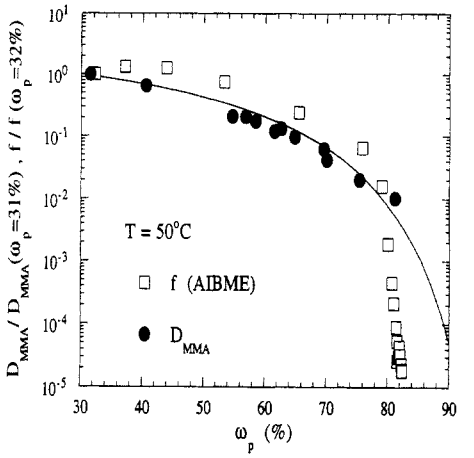

Figure 9. Comparison of the polymer concentration dependence of D_{MMA} with that of f for AIBME. The initiator efficiency values are from ref 61. The solid line is calculated from eqs 5 and 6 using the parameters in Tables 1 and 2. The diffusion coefficient and efficiency data are normalized with respect to their values at $w_p = 31$ and 32%, respectively.

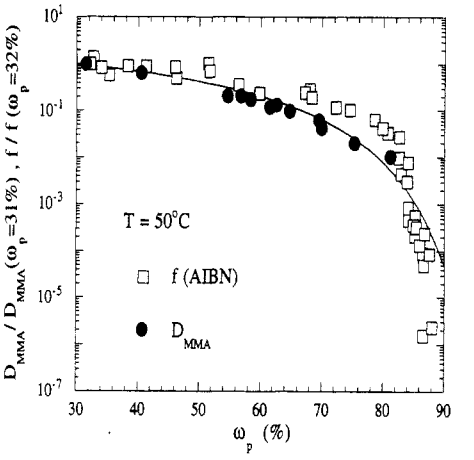

Figure 10. Comparison of the polymer concentration dependence of D_{MMA} with that of f for AIBN. The initiator efficiency data are from ref 19. The solid line is calculated from eqs 5 and 6 using the parameters in Tables 1 and 2. The diffusion coefficient and efficiency data are normalized with respect to their values at $w_p = 31$ and 32%, respectively.

the diffusion coefficient of the ACN fragment, although the latter may have a somewhat stronger concentration dependence than the former. The data in Figure 8 are consistent with the notion that f is controlled by the mobility of the ACN radical.

Estimates of f for AIBME at 50 °C from Adams et al.[62] are compared to D_{MMA} values in Figure 9. The glass transition occurs at $w_{pg} = 89\%$; no data are in the glassy region. The agreement between the diffusion and initiator efficiency data is rather satisfactory, both qualitatively and quantitatively, between 30 and 80% polymer. Subsequently, the decrease in f becomes much steeper than the predictions of the Vrentas–Duda model for D_{MMA}. Most of the decrease of f beyond 80% is likely to arise from the fact that the overall rate of polymerization data used in the calculations show a drastic reduction leading to the limiting conversion. The implications of this observation will be considered below.

The initiator efficiency of AIBN at 50 °C estimated by Russell et al.[19] is compared to D_{MMA} in Figure 10. Entirely similar observations as for the previous case apply. The size ratio of the AIBN radical to MMA is 0.79, following Haward,[51] and therefore a somewhat weaker concentration dependence of f would be expected.

The combined results of Figures 7–10 indicate that the polymer concentration dependence of f can be accounted for by the mobility of molecules with sizes similar to those of the radical fragments formed by the scission of the initiator. Several models of initiation kinetics[18,32,33] report expressions of f that become proportional to the diffusion coefficient of the fragments as the latter quantity decreases with polymer concentration.

The picture of diffusion-controlled initiation has some consequences that can be verified experimentally. One way is to investigate the dependence of f on the initiator concentration. The primary effect of different amounts of initiator on the properties of the polymerization medium is to change the molecular weight of the polymer formed. Since the diffusion of small molecules such as the radical fragments is independent of the polymer molecular weight beyond a certain molecular weight, about 5×10^4 for PMMA, the decrease in the initiator efficiency is expected to be generally independent of the initiator concentration. Both the data of Sack et al.[9] and the calculations of Russell et al.[19] confirm this prediction. Also, since the mobility of small molecules decrease more rapidly with concentration as their size increases, smaller radical fragments will lead to a weaker concentration dependence of f. This difference will be especially emphasized when the polymer concentration is large. The calculations of Russell et al.[19] support this expectation.

The notion that radical recombination is affected by the radical mobility is not new. There have been reports of an increased extent of radical recombination—equivalent to lower f in polymerization—as the viscosity of the surrounding medium was increased, by using either different solvents or polymer solutions.[63–66] In the latter case,[65] it was found that at constant solution viscosity the extent of radical recombination decreases for solutions containing polymers of larger molecular weight. These latter results are consistent with the assumption that radical recombination depends on the mobility of the radicals in the medium. It was shown here that D_{MMA} decreased with polymer concentration but was insensitive to the polymer molecular weight, whereas it is well known that the bulk viscosity increases with both. It follows that a polymer solution of the same viscosity as another containing a smaller polymer will necessarily have a lower concentration and thus the radicals will have a higher diffusion coefficient in the former system, leading to less recombination and, for polymerization, to higher f.

Finally, some of the difficulties mentioned previously will be re-examined in light of the conclusions reached thus far. It was shown that propagation was not controlled by the mobility of MMA, which then demanded an explanation for the decrease in k_p measured in many studies of MMA polymerization. No definitive answer can be given here to the question of the origin of this decrease. Note, however, that the basic experimental observation at intermediate to high conversion is not the decrease of k_p but of the rate of polymerization, R_p, beyond that which can be assigned to monomer and initiator depletion. (In what follows, it is implied that the contribution of reactant depletion has already been included in R_p.) Measurements of R_p determine the group $k_p f^{1/2}$, and not k_p alone; if f is not constant, care must be exercised in extracting both contributions from the measurements in a reliable fashion.

In the absence of a rationale for the decrease in k_p, it may be instructive to consider different causes for the behavior of R_p. Since $R_p \propto k_p f^{1/2}$, it is obvious how a decrease in f can lead to a diminished polymerization rate, even in the case of constant k_p. The measurements of R_p in bulk polymerization can be interpreted in this fashion. Notice, however, that emulsion polymerization arguably proceeds with constant f, but a decrease of R_p has nevertheless been observed.[7] Therefore, in this case, attributing the decrease of R_p solely to f cannot reproduce the experimental observations.

The origin of the limiting conversion must also find an explanation different from diffusion-controlled propagation. A drastic decrease of f could lead to the virtual cessation of polymerization before all monomer is depleted and is thus compatible with the existence of the limiting conversion in MMA bulk polymerization. The calculated values of f in Figures 9 and 10 represent an example of the type of behavior necessary. However, if f is controlled by the mobility of the radical fragments and its concentration dependence is described by that of D_{MMA} to a good approximation, the diffusion data presented here do not show the dramatic decrease that the initiator efficiency would need to have near w_{pg} to account for the rapid decrease of R_p—see Figures 4 and 7–10. Thus, the connection between the limiting conversion and the glass transition cannot be explained by a catastrophic decrease in f near w_{pg} while at the same time maintaining that f is controlled by the mobility of the initiator fragments.

Conclusions

The MMA diffusion coefficient, D_{MMA}, has been determined as a function of polymer concentration, w_p, at different temperatures. The data have been compared to the polymer concentration dependence of the propagation rate coefficient, k_p, and of the initiator efficiency, f, determined during MMA radical polymerization. The concentrations at which MMA/PMMA solutions become glassy have also been determined at different temperatures and compared to the limiting conversion displayed by MMA radical polymerization. Several conclusions have emerged.

(1) The notion of diffusion-controlled propagation is found to be untenable in the range of polymer concentrations for which both D_{MMA} and k_p data are available, including concentrations near the glass transition of the polymerization medium. The measured values of D_{MMA} are much larger than would be necessary to control propagation kinetics. A different explanation must be sought for the decrease in both the overall rate of polymerization and k_p with polymer concentration that has been measured experimentally in many studies.

(2) The concentration dependence of f for three different initiators measured or calculated in recent investigations is well described by the concentration dependence of D_{MMA} in a broad range of polymer concentrations. Since D_{MMA} provides a very good estimate of the diffusion coefficient of the radical fragments produced by the scission of the initiator, this observation supports the concept that the extent of radical recombination is controlled by the mobility of the fragments. Several consequences of this picture are shown to agree, at least qualitatively, with experimental observations and model calculations. Examples are the independence of initiator efficiency on initiator concentration and the lower efficiency at high polymer concentration of initiators that produce larger fragments. In regard to the latter, it should also be noticed that the size of the initiator fragments becomes an additional variable that can be manipulated to influence the course of polymerizations carried to high conversion.

(3) The decrease in f could account for the observed decrease of the rate of bulk polymerization even in the

case of constant k_p. Interpreting the decrease of R_p observed during emulsion polymerization is more difficult, however, since f is arguably constant throughout the course of the reaction.

(4) The limiting conversion was found to correlate well with the polymer concentration at which the system turns into a glass during bulk MMA polymerization. This appears to be the first time this connection has been made using experimental measurements of the glass transition. In light of the preceding conclusions, however, the reason for the correlation is not clear. At the glass transition, D_{MMA} is sufficiently large not to limit k_p and also does not show the dramatic decrease near the glass point that f would need to have to explain a near-zero rate of polymerization.

Acknowledgment. We would like to thank Professors G. Meyerhoff, R. G. Gilbert, and D. J. T. Hill for providing us with tables of their data. The financial support of the Shell Companies Foundation is gratefully acknowledged.

References and Notes

(1) *Comprehensive Chemical Kinetics*; Bamford, C. H., Tipper, C. F. H., Eds.; Elsevier: Amsterdam, 1976; Vol. 14A.
(2) Moad, G.; Rizzardo, E.; Solomon, D. H.; Johns, S. R.; Willing, R. I. *Makromol. Chem., Rapid Commun.* **1984**, *5*, 793.
(3) Buback, M.; Schweer, J. *Z. Phys. Chem.* **1989**, *161*, 153.
(4) Buback, M.; Degener, B.; Huckestein, B. *Makromol. Chem., Rapid Commun.* **1989**, *10*, 311.
(5) Yamada, B.; Kageoka, M.; Otsu, T. *Macromolecules* **1991**, *24*, 5234.
(6) Hayden, P.; Melville, H. *J. Polym. Sci.* **1960**, *43*, 201.
(7) Ballard, M. J.; Gilbert, R. G.; Napper, D. H.; Pomery, P. J.; O'Sullivan, P. W.; O'Donnell, J. H. *Macromolecules* **1986**, *19*, 1303.
(8) Shen, J.; Tian, Y.; Zeng, Y.; Qiu, Z. *Makromol. Chem., Rapid Commun.* **1987**, *8*, 615.
(9) Sack, R.; Schulz, G. V.; Meyerhoff, G. *Macromolecules* **1988**, *21*, 3345. Sack-Kouloumbris, R.; Meyerhoff, G. *Makromol. Chem.* **1989**, *190*, 1133.
(10) Zhu, S.; Tian, Y.; Hamielec, A. E.; Eaton, D. R. *Polymer* **1990**, *31*, 154.
(11) Carswell, T. G.; Hill, D. J. T.; Londero, D. I.; O'Donnell, J. H.; Pomery, P. J.; Winzor, C. L. *Polymer* **1992**, *33*, 137.
(12) Buback, M.; Gilbert, R. G.; Russell, G. T.; Hill, D. J. T.; Moad, G.; O'Driscoll, K. F.; Shen, J.; Winnik, M. A. *J. Polym. Sci., Polym. Chem. Ed.* **1992**, *30*, 851.
(13) Marten, F. L.; Hamielec, A. E. *ACS Symp. Ser.* **1979**, *104*, 43; *J. Appl. Polym. Sci.* **1982**, *27*, 489.
(14) Soh, S. K.; Sundberg, D. C. *J. Polym. Sci., Polym. Chem. Ed.* **1982**, *20*, 1331.
(15) Stickler, M. *Makromol. Chem.* **1983**, *184*, 2563.
(16) Chiu, W. Y.; Carratt, G. M.; Soong, D. S. *Macromolecules* **1983**, *16*, 348.
(17) Achilias, D.; Kiparissides, C. *J. Appl. Polym. Sci.* **1988**, *35*, 1303.
(18) Achilias, D. S.; Kiparissides, C. *Macromolecules* **1992**, *25*, 3739.
(19) Russell, G. T.; Napper, D. H.; Gilbert, R. G. *Macromolecules* **1988**, *21*, 2141.
(20) Schulz, G. V. *Z. Phys. Chem.* **1956**, *8*, 290.
(21) Burnett, G. M.; Duncan, G. L. *Makromol. Chem.* **1962**, *51*, 154.
(22) Horie, K.; Mita, I.; Kambe, H. *J. Polym. Sci., Part A-1* **1968**, *6*, 2663.
(23) Kelley, F. N.; Bueche, F. *J. Polym. Sci.* **1961**, *50*, 549.
(24) Frick, T. S.; Huang, W. J.; Tirrell, M.; Lodge, T. P. *J. Polym. Sci., Polym. Phys. Ed.* **1990**, *28*, 2629.
(25) Schulz, G. V.; Harborth, G. *Makromol. Chem.* **1947**, *1*, 106.
(26) Balke, S. T.; Hamielec, A. E. *J. Appl. Polym. Sci.* **1973**, *17*, 905.
(27) Stickler, M.; Panke, D.; Hamielec, A. E. *J. Polym. Sci., Polym. Chem. Ed.* **1984**, *22*, 2243.
(28) Zhu, S.; Hamielec, A. E. *Macromolecules* **1989**, *22*, 3093.
(29) Brooks, B. W. *Proc. R. Soc. London, A* **1977**, *357*, 183.
(30) Robertson, E. R. *Trans. Faraday Soc.* **1956**, *52*, 426.
(31) De Schrijver, F.; Smets, G. *J. Polym. Sci., Part A-1* **1966**, *4*, 2201.
(32) Shen, J.; Tian, Y.; Wang, G.; Yang, M. *Sci. China B* **1990**, *33*, 1046.
(33) Arai, K.; Saito, S. *J. Chem. Eng. Jpn.* **1976**, *9*, 302.
(34) Acheson, R. M.; Barltrop, J. A.; Hichens, M.; Hichens, R. E. *J. Chem. Soc.* **1961**, 650.
(35) Hermann, H.; Luttke, W. *Chem. Ber.* **1968**, *101*, 1708, 1715.
(36) Faldi, A. Ph.D. Thesis, University of Minnesota, 1992.
(37) Ehlich, D.; Sillescu, H. *Macromolecules* **1990**, *23*, 1600.
(38) Eichler, H. J.; Günter, P.; Pohl, D. W. *Laser-Induced Dynamic Gratings*; Springer-Verlag: Berlin, 1986.
(39) Sillescu, H.; Ehlich, D. *Lasers in Polymer Science and Technology*; Fouassier, J.-P., Rabek, J. F., Eds.; CRC Press: Boca Raton, FL, 1990; Vol. III.
(40) Stejskal, E. O.; Tanner, J. E. *J. Chem. Phys.* **1965**, *42*, 288.
(41) von Meerwall, E.; Burgan, R. D.; Ferguson, R. D. *J. Magn. Reson.* **1979**, *34*, 339.
(42) von Meerwall, E.; Ferguson, R. D. *J. Appl. Polym. Sci.* **1979**, *23*, 877.
(43) von Meerwall, E.; Grigsby, J.; Tomich, D.; Van Antwerp, R. *J. Polym. Sci., Polym. Phys. Ed.* **1982**, *20*, 1037.
(44) von Meerwall, E.; Ferguson, R. D. *Comput. Phys. Commun.* **1981**, *21*, 421. This software has been continuously improved by the inclusion of new features and converted to operate on UNIX and MS-DOS workstations.
(45) von Meerwall, E.; Kamat, M. *J. Magn. Reson.* **1989**, *83*, 309.
(46) von Meerwall, E.; Palunas, P. *J. Polym. Sci., Polym. Phys. Ed.* **1987**, *25*, 1439.
(47) Vrentas, J. S.; Duda, J. L. *J. Polym. Sci., Polym. Phys. Ed.* **1977**, *15*, 403, 417, 441.
(48) Ferguson, R. D.; von Meerwall, E. *J. Polym. Sci., Polym. Phys. Ed.* **1980**, *18*, 1285.
(49) Huang, W. J.; Frick, T. S.; Landry, M. R.; Lee, J. A.; Lodge, T. P.; Tirrell, M. *A.I.Ch.E. J.* **1987**, *33*, 573.
(50) Vrentas, J. S.; Duda, J. L.; Ling, H.-C.; Hou, A.-C. *J. Polym. Sci., Polym. Phys. Ed.* **1985**, *23*, 289.
(51) Haward, R. N. *J. Macromol. Sci., Rev. Macromol. Chem.* **1970**, *C4*, 191.
(52) Rogers, S. S.; Mandelkern, L. *J. Phys. Chem.* **1957**, *61*, 985.
(53) Stickler, M.; Panke, D.; Wunderlich, W. *Makromol. Chem.* **1987**, *188*, 2651.
(54) Chapiro, A. *Eur. Polym. J.—Suppl.* **1969**, 43.
(55) Wunderlich, W. In *Polymer Handbook*, 3rd ed.; Brandrup, J., Immergut, E. H., Eds.; John Wiley & Sons: New York, 1989, p V-77.
(56) Cowie, J. M. G. *Eur. Polym. J.* **1975**, *11*, 297.
(57) Smoluchowski, M. *Z. Phys. Chem.* **1918**, *92*, 129.
(58) Allen, P. E. M.; Patrick, C. R. *Makromol. Chem.* **1961**, *47*, 154.
(59) Gebert, M. S.; Yu, D. H.-S.; Torkelson, J. M. *Macromolecules* **1992**, *25*, 4160.
(60) Radical polymerization produces PMMA with a glass transition temperature equal to 105 °C. This value is different from the glass transition temperature of 119 °C measured for the PMMA samples used in this work, which were prepared by anionic polymerization. The other parameters in eq 7 are assumed to be the same for the two types of PMMA.
(61) Li, W.-H.; Hamielec, A. E.; Crowe, C. M. *Polymer* **1989**, *30*, 1513.
(62) Adams, M. E.; Casey, B. S.; Mills, M. F.; Russell, G. T.; Napper, D. H.; Gilbert, R. G. *Makromol. Chem., Macromol. Symp.* **1990**, *35/36*, 1.
(63) Dobis, O.; Pearson, J. M.; Szwarc, M. *J. Am. Chem. Soc.* **1968**, *90*, 278.
(64) Chakravorty, K.; Pearson, J. M.; Szwarc, M. *J. Am. Chem. Soc.* **1968**, *90*, 283.
(65) Niki, E.; Kamiya, Y. *J. Am. Chem. Soc.* **1974**, *96*, 2129.
(66) Valiquette, G.; Weir, N. A. *J. Chem. Soc.* **1972**, 1071.